Modulating expression level of secreted Wnt3 influences cerebellum development in zebrafish transgenics

Cathleen Teh[1#], Guangyu Sun[2,3#], Hongyuan Shen[1], Vladimir Korzh[1,4*], Thorsten Wohland[2,3,4*]

1-Institute of Molecular and Cell Biology, Agency for Science, Technology and Research, Singapore;

2 - Department of Chemistry, National University of Singapore, Singapore;

3 - Center for Bioimaging Sciences, National University of Singapore, Singapore;

4 - Department of Biological Sciences, National University of Singapore, Singapore.

Running title: Secreted Wnt3 influences cerebellum patterning

Key words: fluorescence correlation spectroscopy (FCS), cerebellum, brain ventricle, protein fractions, ligand, C59 Wnt inhibitor.

#- Equal contribution

*Corresponding authors:

Vladimir Korzh (vlad@imcb.a-star.edu.sg; zebrafish transgenics),

Thorsten Wohland (twohland@nus.edu.sg; FCS)

SUMMARY

The boundaries of brain regions are associated with the tissue-specific secretion of ligands from different signalling pathways. The dynamics of these ligands *in vivo* and the impact of its disruption remain largely unknown. We used light and fluorescence microscopy for the overall imaging of the specimen and fluorescence correlation spectroscopy (FCS) to determine Wnt3 dynamics and demonstrated that Wnt3 regulates cerebellum development during embryogenesis using zebrafish Wnt3 transgenics with either tissue-specific expression of an EGFP reporter or a functionally active fusion protein, Wnt3EGFP. The results suggest a state of dynamic equilibrium of Wnt3EGFP mobility in polarized neuroepithelial-like progenitors in the dorsal midline and cerebellar progenitors on the lateral side. Wnt3EGFP secretes from the cerebellum as shown by measurements of its mobility in the ventricular cavity. The importance of Wnt secretion in brain patterning was validated with the Porc inhibitor Wnt-C59 (C59), which applied early reduced membrane-bound and secreted fractions of Wnt3EGFP and led to a malformed brain characterized by the absence of epithalamus, optic tectum and cerebellum. Likewise, interference with Wnt secretion later on during cerebellar development negatively impacted cerebellar growth and patterning. Our work supported by quantitative analysis of protein dynamics *in vivo*, highlights the importance of membrane localized and secreted Wnt3 during cerebellum development.

INTRODUCTION

As the brain develops, cell proliferation becomes restricted to a vicinity of several signaling centers. Their signaling function and brain development henceforth are mediated by secreted ligands of several signaling pathways (Ye et al., 1998; Ye et al., 2001). The brain midline is one of the signaling centers represented dorsally by the roof plate and ventrally by the floor plate. These cells, along with those of the mid-diencephalic and mid-hindbrain boundaries, represent the signaling glia, which is a source of secreted factors, including Wnts involved in the dorso-ventral (D-V) and antero-posterior (A-P) specification of the brain (Jessell, 2000; Korzh et al., 2007). The signaling glia having extended soma and/or filopodia, functions as a conduit of distant delivery of hydrophobic Wnts (Kondrychyn et al., 2013; Korzh, 2014; Stanganello et al., 2015).

Several zebrafish Wnt genes are expressed at the midbrain-hindbrain boundary (MHB) and roof plate (Molven et al., 1991; Krauss et al., 1992; Blader et al., 1996). Mutations affecting Wnt signaling in zebrafish illustrated an important role of canonical Wnt/β-catenin signaling during neural development (Dorsky et al., 2002; Bonner et al., 2008). Wnt signaling is required for normal brain development (Clevers and Nusse, 2012), including that of the cerebellum (Selvadurai and Mason, 2011). Cerebellar vermis hypoplasia in Joubert syndrome for example is linked to defective canonical Wnt signaling (Lancaster et al., 2011). Wnt3 is expressed in the developing cerebellum and the dorsal spinal cord of all vertebrates (Roelink and Nusse, 1991; Bulfone et al., 1993; Garriock et al., 2007; Clements et al., 2009; Anne et al., 2013). In mice Wnt3 is expressed prior to gastrulation and its targeted deletion causes an early developmental arrest (Liu et al., 1999). In human, homozygous nonsense mutation within the WNT3 coding region (Q83X) resulted in the loss of all limbs with concomitant CNS, craniofacial and

urogenital defects in affected fetuses (Niemann et al., 2004). WNT3 was identified as an extracellular regulator of granule cell progenitor proliferation and differentiation during mouse cerebellar development (Anne et al., 2013). Depending on cellular context Wnt3 either acts via the canonical Wnt pathway by activating the nuclear translocation of β-catenin (Kim et al., 2008) or via the RhoA pathway (Kobune et al., 2007).

Secretion of Wnts is of particular interest due to a role of excessive production of Wnts in oncogenesis (Nusse and Varmus, 1982; Nusse and Varmus, 2012). Assessing the level of Wnt activity and modulating these activities *in vivo* can be achieved using a combination of fluorescent transgenic reporters and inhibitors of Wnt signaling (Yin et al., 2012; Anastas and Moon, 2013; Proffitt et al., 2013). To study a role of Wnt3 in development, the zebrafish *wnt3* transgenics expressing the Wnt3-EGFP fusion protein or EGFP reporter under control of 4 kb *wnt3* promoter were generated, which express either transgenes in the developing cerebellum. This opened a possibility to investigate Wnt3 mobility *in vivo* using fluorescence correlation spectroscopy (FCS) as shown for teleost embryos (Pan et al., 2007b; Ries et al., 2009) and the *Drosophila* wing (Zhou et al., 2012). Results obtained from FCS analysis include determination of diffusion coefficients in cytosolic as well as membrane-associated fractions of EGFP-labeled proteins (Shi et al., 2009; Yu et al., 2009; Muller et al., 2013). Same approach was used here to define the intracellular and extracellular populations of Wnt3 and effects of two different Wnt inhibitors [C59 - (Proffitt et al., 2013; Stewart et al., 2014)] and [IWR-1 - (Lu et al., 2009; Yin et al., 2012)] on Wnt3 populations distribution and function. The aim of this research is to study protein dynamics *in vivo* (Pan et al., 2007a; Mütze et al., 2011; Foo et al., 2012; Machan and Wohland, 2014) and associate it with cerebellum development/growth. Our results demonstrate

the importance of membrane-localized and secreted Wnt3 in regulation of cerebellar development.

RESULTS

Tg(*wnt3*:EGFP) is a faithful reporter of Wnt3 expression

The expression pattern of zebrafish *wnt3* has been described (Clements et al., 2009). To begin deciphering the role of Wnt3 in neural development, two DNA regulatory fragments, 2kb and 4kb in length, 5' upstream from the translational start site of *wnt3* were PCR amplified using the zebrafish BAC (CR450820.4) as a template. The PCR product was sub-cloned into a promoterless EGFP vector (pEGFP-1). Transient transgenesis carried out by panembryonic injection of either plasmid into 1-2 cell stage zebrafish embryos detected promoter activity from the 4kb fragment. The transgenic lines were generated using the modified Tol2 transposon system. The 4kb-EGFP fragment was sub-cloned into the miniTol2 vector (Balciunas et al., 2006) and injected into embryos. Several independent transgenic lines differing in the intensity of EGFP expression with expression pattern similar to that of *wnt3* were generated. Here we used Tg(-4.0*wnt3*:EGFP)^{F1} transgenics.

To determine whether Tg(-4.0*wnt3*:EGFP)^{F1} faithfully reports *wnt3* transcription at different developmental stages, we compared *in vivo* images of EGFP expression with that of *wnt3* between 24 to 72 hpf (Figure 1A). The spatial-temporal profile of EGFP expression in the ventral epithalamus, roof plate, optic tectum, floor plate, MHB, cerebellum (ce) and hindbrain closely mimics that of *wnt3* (24-72 hpf; Figure 1A-J). The co-immunohistochemical detection of EGFP and the neuronal marker HuC/D on cross sections of 48 hpf embryos (Figure 1G-J) indicated that EGFP(+) domains in the roof plate, tegmental floor plate and cerebellum are

flanked by HuC/D-positive neurons and do not express this differentiation marker. This suggests that EGFP-expressing cells are committed to a non-neuronal fate. Hence the 4 kb *wnt3*-promoter contains most if not all regulatory elements and allows *in vivo* detection of Wnt3 expression.

Wnt3EGFP is expressed in domains of endogenous *wnt3*

To facilitate the analysis of Wnt3 function *in vivo* the same promoter was used to generate transgenics expressing the functionally active Wnt3 fusion protein (Wnt3EGFP). The functional activity of the fusion protein was first verified in zebrafish embryos. The *wnt3*:*egfp* fusion cassette was cloned downstream of the constitutively active cytomegalovirus (CMV) promoter. The panembryonic overexpression of this construct led to malformed eyes and posteriorized CNS, i.e. the phenotype associated with ectopic Wnt signalling (van de Water et al., 2001). This indicated that the recombinant Wnt3EGFP retains Wnt3 activity (Figure S1A).

The CMV promoter was replaced with the 4kb *wnt3* promoter and the resulting construct (-4.0*wnt3*:Wnt3EGFP) was used to generate zebrafish transgenics [eg. Tg(-4.0*wnt3*:Wnt3EGFP)^{F1} and Tg(-4.0*wnt3*:Wnt3EGFP)^{F2}] with spatial temporal expression of EGFP identical to that in the reporter line Tg(-4.0*wnt3*:EGFP)^{F1} (Figure 2A-O). This expression is temporally regulated. Both EGFP and Wnt3EGFP were first detected in polarized neuroepithelial cells of the dorsal midline in the optic tectum, cerebellum and the cerebellar rhombic lip, one of the germinal zones in the cerebellum (Hashimoto and Hibi, 2012); Figure 2A; F; K). Both expression are enhanced by 36 hpf and reduces by 4 days post fertilization (dpf; Figure 2P-V). The only exception is Tg(-4.0*wnt3*: Wnt3EGFP)^{F3} where expression started relatively late (36 hpf) and remains high in the developing cerebellum (Figure 2W). The four different transgenic lines of zebrafish expressing EGFP or Wnt3EGFP fusion protein in the cerebellum are referred to as Tg(*wnt3*:EGFP)^{F1};

Tg(*wnt3*:Wnt3EGFP)^{F1}; Tg(*wnt3*:Wnt3EGFP)^{F2}; Tg(*wnt3*:Wnt3EGFP)^{F3} in the rest of this manuscript.

Functional Wnt3EGFP positively regulates flanking tissues growth in the MHB and the cerebellum

The impact of spatiotemporal control of Wnt3 dosage on flanking tissues growth was assessed in living zebrafish using Tg(memKR15-16), expressing the membrane-tethered fluorescent protein KillerRed (KR). This transgenic line trapped the expression of the zebrafish *eng1b* (Kondrychyn et al., 2011), an orthologue of the mouse *En-1*. Both Wnt-3 and En-1 transcripts are detected in the embryonic mouse MHB and the cerebellum (Millen et al., 1995). Similarly in the *eng1b* trapped transgenic zebrafish, KillerRed expression in the MHB and the cerebellum overlaps with and flanks Wnt3EGFP expression in Tg(*wnt3*:Wnt3EGFP) families. Histological characterization of Tg(*wnt3*:Wnt3EGFP)^{F2} in the background of Tg(memKR15-16) confirmed Wnt3EGFP expression in the cerebellum, where Wnt3EGFP cells are predominantly localized to the upper rhombic lip (Figure S2D-G), a proliferative niche containing progenitor cells even in adult fish (Kaslin et al., 2013). Most of Wnt3EGFP detected by immuno-histochemistry accumulates in the plasma membrane of expressing cells, mimicking that detected in transgenics *in vivo*. All of Wnt3EGFP-positive cells of cerebellum are negative for the neuronal marker HuC/D at 3dpf (Figure S2D-E). All Wnt3EGFP-expressing cells in the ventral MHB adopt the distinct radial glia-like morphology with cell bodies located within the luminal aspect of the ventricular wall and a primary process extending into the subventricular zone (Figure S2B-C; F-G). The glial identity of these cells is confirmed by immunodetection of glial fibrillary acidic protein (GFAP). Co-localization of some Wnt3EGFP cells with BrdU-positive replicating cells (Figure S2F-G) in the cerebellum confirms their localization to a proliferation niche.

Wnt3's role in inhibiting proliferation of cultured cerebellar granule progenitors and regulating its neurogenesis was documented in mice (Anne et al., 2013). We asked whether a similar role exists for Wnt3 by assessing the impact on cerebellum neurogenesis in zebrafish. In the absence of a zebrafish *wnt3* mutant, the functional analysis was conducted using the morpholino phosphodiamidate antisense oligonucleotides (MO)-mediated loss-of-function (LOF) approach. Knockdown of Wnt3 was achieved by interfering with pre-mRNA splicing at the exon1-intron1 boundary (MO1) or inhibition of mRNA translation by targeting *wnt3* 5'-UTR (MO2, Figure S3A). RT-PCR with *wnt3*-specific primers showed that microinjection of MO1 successfully interfered with *wnt3* splicing such that no wild type *wnt3* transcripts could be detected in 30 hpf embryos after MO1 injection (Figure S3B). MO2 anneals to the 25 bp sequence in the *wnt3* 5'-UTR. This sequence is also present in the 4kb *wnt3* upstream promoter that drives reporter expression in Wnt3 stable transgenics. The specificity of MO2 was verified by microinjecting into Tg(*wnt3*:EGFP)^{F1} where interference of EGFP translation upon binding of MO2 to *wnt3* 5'-UTR upstream of the EGFP reporter was documented. EGFP intensity is similar in wild type (WT) controls and Tg(*wnt3*:EGFP)^{F1} MO1 morphants (Figure S3C-E), but reduced in MO2 morphants (Figure S3F-G). To eliminate undesirable off-target effects (Robu et al., 2007) of *wnt3* MOs, concurrent p53 and Wnt3 knockdown was performed. The effect of Wnt3 knockdown on cerebellar neurogenesis was examined using the zebrafish HuC transgenics, Tg(*elav3*:GFP). GFP in these transgenics labels all neurons (Park et al., 2000). GFP expression in both WT and Wnt3 morphants at 3dpf (Figure S3H-L) were compared and microinjection of either MO1 or MO2-morphants, with or without p53 MO consistently reduces GFP-positive neurons in the cerebellum (enlarged white box) of Tg(*elav3*:GFP) morphants. This suggests that zebrafish *wnt3* plays an essential role in cerebellar neurogenesis.

We further investigated the impact of Wnt3 dosage on cerebellum development. The cerebellum located at the dorsal-most part of the anterior hindbrain is posterior to MHB. Volumetric assessment of *eng1b*-trapped MHB and cerebellum in Tg(*wnt3*:EGFP) or Tg(*wnt3*:Wnt3EGFP) families was performed to determine an impact of Wnt3 dosage on growth of KR-marked domains in Tg(memKR15-16) transgenics (Figure 3A-C). The double transgenics of Tg(memKR15-16)/Tg(*wnt3*:EGFP)^{F1} was used as a control group expressing normal level of Wnt3. Double transgenic larvae of Tg(*wnt3*:Wnt3EGFP)^{F2} represent the group with intermediately elevated Wnt3 expression and Tg(*wnt3*:Wnt3EGFP)^{F3} represents the group with high Wnt3 expression. Volumetric analysis of the KR-positive brain segment (MHB and cerebellum) at 4 dpf demonstrated that Tg(*wnt3*:Wnt3EGFP)^{F3} has on average a 22% larger memKR-positive domain comparing to controls (Figure 3D; P=0.0022). The positive correlation between *in vivo* Wnt3EGFP dosage and brain volume suggests that Wnt3EGFP is functional and positively regulates growth of the MHB and cerebellum.

The ability of bioactive Wnt3EGFP to compensate endogenous Wnt3 activity after MO1 meditated knockdown was confirmed in double transgenics of Tg(memKR15-16) larvae expressing either EGFP or Wnt3EGFP (Figure 4). Where Tg(*wnt3*: Wnt3EGFP)^{F3} expresses endogenous Wnt3 and Wnt3EGFP. The Wnt3 reporter Tg(*wnt3*:EGFP)^{F1} is the control group expressing only endogenous Wnt3. Since MO1 interferes with the formation of mature *wnt3* transcripts in all injected larvae, the cerebellum in Tg(*wnt3*:EGFP)^{F1} and Tg(*wnt3*:Wnt3EGFP)^{F3} Wnt3 morphants are significantly smaller than un-injected siblings [($P<0.0001$) and ($P=0.0034$), correspondingly]. Nevertheless, Wnt3 morphants of Tg(*wnt3*:Wnt3EGFP)^{F3} have a significantly bigger cerebellum than Tg(*wnt3*:EGFP)^{F1} counterparts (Figure 4I, P= 0.0003) due to additional Wnt3EGFP expression in the cerebellum. We further assessed whether decreased brain volume

observed in Wnt3 morphants is attributed to a change in cell size or cell numbers. Same sample sets were concurrently analyzed for cell size (cell area), taking 10 random cells from a morphologically similar optical slice of the cerebellum. Cell area was measured using Image J software. No significant difference in cell size (Figure S4) was detected in Wnt3 morphants when compared to controls. Clear difference in area/cell numbers of the KR-labelled optical slice correlated with quantitated volume presented in Figure 4. Hence Wnt3 linked changes in cerebellum volume results in alteration of cell numbers rather than cell size.

Characterization of Wnt3EGFP membrane dynamics *in vivo*

Wnt3EGFP must be secreted in a manner comparable to endogenous Wnt3 to function properly. Confocal microscopy showed that Wnt3EGFP has been transported to the plasma membrane. FCS was instrumental to determine diffusion coefficients of cytosolic as well as membrane tethered EGFP-labeled proteins (Shi et al., 2009). The mobility of secreted ligands in the extracellular space could be involved in generating the morphogen gradient in developing zebrafish (Yu et al., 2009). Hence we decided to characterize the distribution of Wnt3EGFP at the plasma membrane using FCS. Tg(*wnt3*:Wnt3EGFP)^{F2} transgenic embryos were used to detect Wnt3EGFP by FCS in the cerebellum. Figure 5A shows a typical autocorrelation curve measured on the plasma membrane. The experimental data was fitted with a model, which was determined by Bayes inference-based model selection (Guo et al., 2012; Sun et al., 2015). The model accounts for two diffusive particles and also a possible triplet state of the fluorophore (equation 13 in M&M). A significant fraction of the protein detected (60%, fraction F_2) was represented by a membrane-tethered component with a diffusion coefficient (D_2) ~ 1 $\mu m^2/s$. This fraction could be present either in cells secreting Wnt3 and/or in cells receiving Wnt3. The rest of the signal (40%) was represented by a fast moving component with diffusion coefficient D_1 ~

30 μm^2/s. This fast moving component is similar to the cytosolic EGFP in Tg(-4.0*wnt3*:EGFP)^{F2} (abbreviated EGFP^{F2}, see Table S1). A lower diffusion coefficient is expected because of the difference in molecular mass of Wnt3EGFP and cytosolic EGFP. In addition, considering the possibility of posttranslational modification of Wnts by lipids, the fast component could be in a soluble complex with other partner(s) (Willert et al., 2003) further lowering the diffusion coefficient.

We tested whether the protein dynamics varies in different parts of the cerebellum such as between polarized neuroepithelial-like progenitors in the dorsal midline (DM) and cerebellar progenitors on the lateral side (LS) during development. Measurements were performed in these two regions (DM and LS) at 28, 34 and 48 hpf (Figure S5A). The results showed that Wnt3EGFP mobility and its membrane distribution (F_2) in Tg(*wnt3*:Wnt3EGFP)^{F2} remains relatively constant in both regions of the cerebellum throughout this period (Figure S4C-E). The data were also analyzed for cells with different expression levels selected based on fluorescence intensity, but no significant difference in Wnt3EGFP membrane distribution (F_2) was detected (Figure S5F). These data suggest that Wnt3 fractions are in a stable dynamic equilibrium during cerebellum development.

As a negative control, we also assayed the distribution of LynEGFP, a tracer membrane-tethered protein, which being non-secreted remains in the cell. Compared to Wnt3EGFP, the mobility of both the fast- and slow-moving components of LynEGFP are on the same order of magnitude although slightly higher (Figure 5B and 5C). This suggested that the fast Wnt3 component represents intracellular Wnt3EGFP. Since during this period of development the nucleus occupies most of the cell volume both components are detected near the plasma membrane (Figure S5B). The expression level does not influence LynEGFP dynamics similar to that of

Wnt3EGFP (Figure S5F). However, the membrane fraction (F_2) of Wnt3EGFP is approximately 5% less than that in LynEGFP (Figure 5D and Figure S5F) suggesting that this amount probably represents secreted Wnt3EGFP. To analyze this fraction we measured Wnt3EGFP in the brain ventricle adjacent to Wnt3-expressing cells.

Characterization of Wnt3EGFP dynamics in the brain ventricle

The small extracellular space in the tissue makes it difficult to further characterize the extracellular fraction of Wnt3EGFP. Fortunately, the 4th brain ventricle is directly adjacent to Wnt3-expressing cells in the cerebellar rhombic lip. Hence we analyzed changes in fluorescence intensity at an axis perpendicular to the border of the cerebellum into the fourth ventricle in animals expressing the Wnt3EGFP, LynEGFP or secreted version of EGFP (secEGFP; Figure 6A and Figure S6). Measurements along this axis from the cerebellum boundary into the brain ventricle were performed along the white arrow (Figure 6B). The intensity was normalized to the highest point, which for Wnt3EGFP- and LynEGFP-expressing cells corresponds to the plasma membrane. To show a distribution of secreted proteins, the secEGFP was used as a marker in combination with KillerRed (see Materials and Methods) where membrane-tethered KillerRed expression in the cerebellum of Tg(memKR15-16) demarcates the cerebellum boundary (Kondrychyn et al., 2011) flanking the brain ventricle. The profile of secEGFP distribution was normalized to the average intensity in the brain ventricle (see details in M&M). In parallel it was also found that the Wnt3EGFP is secreted and released into the brain ventricle unlike LynEGFP (Figure 6C). Consistent with previously estimated low level secretion inferred from the membrane distribution in Tg(*wnt3*:Wnt3EGFP)^{F2}, a moderate but significant increase of Wnt3EGFP fluorescence was observed in the brain ventricle unlike LynEGFP. Furthermore, FCS was applied to determine the extracellular mobility of Wnt3EGFP by measurements in the

brain ventricle at a distance of 100 μm from the cerebellum edge. The autocorrelation curves show that the Wnt3EGFP diffuses freely, i.e. similar to that of the secEGFP, whereas no fluorescence in this area was detected in the LynEGFP or negative control embryos (Figure 6D). These results confirm secretion of the Wnt3EGFP into the brain ventricle and support the existence of the extracellular fraction of Wnt3EGFP.

FCS was used to measure the protein mobility in different regions of the brain (Figure 6E and Table S2). The mobility of secEGFP measured in the cerebellum largely represents that of extracellular protein, which is on average 50% lower compared to the mobility of Wnt3EGFP secreted into the brain ventricle. The values defining the mobility of cytosolic EGFP and that of the fast-moving component of LynEGFP represent the mobility of intracellular protein, which is slightly lower than that of extracellular protein. In addition, an extra slow component of Wnt3EGFP with diffusion coefficients 0.5 – 15 $\mu m^2/s$ was detected in the brain ventricle (Figure S6B). This component represented 3 – 30% of all Wnt3EGFP (Figure S7C). This is in contrast to secEGFP, which exhibited only a single component in the brain ventricle (Guo et al., 2012; Sun et al., 2015). Measurements of Wnt3EGFP mobility in the ventricular cavity not only supported the idea of a secreted fraction, but also demonstrated its release from the plasma membrane of Wnt3EGFP (+) cerebellar progenitors into the flanking 4^{th} brain ventricle. In addition, these results support the presence of a very slow-migrating secreted fraction. Thus, these measurements demonstrate the presence of three fractions of Wnt3EGFP, a fast-migrating intracellular fraction, a slow-migrating membrane fraction and a secreted fraction, which itself consists of a fast- and a slow-migrating components.

Block of Porcupine affects Wnt3EGFP secretion

It has been reported that Porcupine (Porc), a membrane-bound O-acyl transferase, is necessary for Wnts anchoring to the cell membrane in Wnt-producing cells (Tanaka et al., 2000). In absence of Porc activity, Wnts are less hydrophobic and accumulate in the endoplasmic reticulum (ER). We used the Porc inhibitor Wnt-C59 (C59) to reveal the role of Wnt secretion in formation of distinct intra- and extracellular fractions of Wnt3EGFP. In parallel, IWR-1, another inhibitor of Wnt signaling acting at the level of activity of *β*-catenin in target cells, and thus not influencing secretion was used for in vivo comparison of inhibitor action (Chen et al., 2009; Lu et al., 2009).

First, Tg(*wnt3*:Wnt3EGFP)^{F2} embryos were soaked in 20 μM of C59. This blocked formation of cerebellum and strongly reduced Wnt3EGFP (unpublished observations). This is in line with characteristics of C59 as an inhibitor of Wnt secretion (Proffitt et al., 2013). To perform FCS, a minimal level of Wnt3EGFP expression is required. Hence for FCS experiments the concentration of C59 was reduced to 5 μM. The number of Wnt3EGFP expressing cells and the level of Wnt3EGFP expression were significantly reduced (Figure 7A), while retaining sufficient Wnt3EGFP for FCS. As a control, the LynEGFP transgenics with expression in the cerebellum; Tg(*-8.0cldnB:*lynEGFP), were used (Figure 7B) along with the control (untreated) and 1% DMSO-treated Tg(*wnt3*:Wnt3EGFP)^{F2} embryos. C59 has no effect on distribution of LynEGFP. In particular, the mobility of both fast- and slow-migrating components (D_1 and D_2) as well as the membrane distribution (F_2) of LynEGFP were not affected by this treatment (Figure 7C-E), indicating that properties of plasma membrane are not affected. In contrast, Wnt3EGFP mobility on the membrane (D_2) and its membrane distribution (F_2) varied significantly; D_2 increased two-fold and F_2 was reduced approximately 15% compared to controls (Figure 7D-E) and Wnt3EGFP is almost absent in the brain ventricle (Figure S8). In contrast, Wnt3EGFP

expression and/or its secretion were not affected even at high concentration of IWR-1 inhibitor (50 μM, Table S3, Figure S8). The impact of C59-mediated Wnt inhibition on brain patterning is confirmed using double transgenic Tg(*wnt3*:Wnt3EGFP)^{F2}/Tg (memKR15-8) larvae where membrane tethered KillerRed demarcates specific segments of the brain (epithalamus, optic tectum, cerebellum and hindbrain). Successful interference with Wnt secretion by C59 during primary neurulation, first detected by FCS at 28hpf, correlated with a drastic reduction of Wnt3EGFP and a malformed brain characterized by the absence of epithalamus, optic tectum and cerebellum at 48 hpf (Figure S9D). Therefore, FCS data support the hypothesis that the ratio of various fractions of Wnt3EGFP depends on efficiency of its secretion. Inhibition of Wnt secretion causes an increase of the intracellular fraction of Wnt3EGFP and a reduction of its membrane-bound fraction. The latter consequently led to defective morphological patterning of the brain confirmed 1 day after the initial FCS analysis.

Inhibition of cerebellar Wnt3EGFP secretion reduces its segmental volume

We wanted to validate whether interference with Wnt secretion during cerebellar development negatively impacts cerebellar growth and patterning. Tg(*wnt3*:Wnt3EGFP)^{F3}/Tg(memKR15-16) double transgenic larvae are selected as they have the highest Wnt3EGFP expression resulting in the largest brain increase (Figure 3C). Embryos were exposed to Wnt inhibitors at 36 hpf, after the onset of Wnt3EGFP expression in Tg(*wnt3*:Wnt3EGFP)^{F3} and treatment stopped at 72hpf. The EGFP reporter represents embryos with endogenous level of Wnt3, i.e. negative control (Figure 8A). Tg(*wnt3*:Wnt3EGFP)^{F3} embryos treated by 1%DMSO represent a positive control (Figure 8B). Embryos were treated with Wnt inhibitors (C59 or IWR1) by whole embryo soaking (Figure 8C-D). Wnt3 activity is required after 36 hpf for cerebellar development since exposure to either C59 (Figure 8C) or IWR-1 (Figure 8D) resulted in brain reduction. The

decrease caused by IWR is small (~9%) unlike that caused by C59, where the cerebellum size was reduced by almost half (P=0.0001) when compared to the positive control (Figure 8E). This decrease in brain segmental volume is accompanied by accumulation of Wnt3EGFP in cells (Figure 8C).

DISCUSSION

Wnt3 is one of about 20 ligands acting in the Wnt signaling pathway implicated in cell proliferation, differentiation and disease. It is expressed by several signaling centers of the neural tube, including, but not limited to the roof plate, floor plate, MHB and mid-diencephalic boundary (Clements et al., 2009). In the brain these domains encircle a large block of tissue encompassing the posterior diencephalon, midbrain and cerebellum. But could an influence of this secreted factor be experienced beyond this area? The brain ventricles adjacent to the domains of Wnt3 secretion present a possibility to spread this secreted ligand in the cerebrospinal fluid (CSF) over all ventricular and central canal surfaces. The zebrafish transgenics expressing the marker EGFP in agreement with expression pattern of *wnt3* validated tissue-specific activity of the *wnt3* promoter (Figure 1). The same promoter was used to generate three stable transgenic zebrafish lines expressing the functionally active fusion Wnt3EGFP protein in a tissue-specific manner (Figure 2). The viable EGFP and the Wnt3EGFP transgenic lines permit faithful tracking of Wnt3 expression and *in vivo* characterization of its function. Conserved spatiotemporal dynamics of Wnt3EGFP fusion protein in Tg(*wnt3*:Wnt3EGFP)^{F2} shared with characterized EGFP reporter line Tg(*wnt3*:EGFP)^{F1} allow FCS studies of Wnt3EGFP mobility and distribution to be carried out in a manner similar to that of endogenous Wnt3.

The FCS measurements in Wnt3EGFP transgenics demonstrated the presence of several fractions of Wnt3EGFP (Figure 9A), including two intracellular fractions - i) fast-migrating intracellular fraction, ii) slow-migrating membrane fraction, and two secreted fractions: iii) fast-migrating diffusing fraction and, iv) very slow-migrating one. The bulk of Wnt3EGFP is represented by intracellular fractions, which are difficult to resolve in space due to a relatively thin layer of cytoplasm in developing cells. In contrast, FCS provides a possibility to resolve fractions of different molecular mass by measuring mobility of proteins and their complexes. This led to characterization of the fast-migrating and slow-migrating fractions of Wnt3EGFP. The former probably represents the cytosolic fraction, and possibly some Wnt3 secreted into the extracellular space. This assumption is based on the fact that the fraction of fast-migrating proteins is larger for Wnt3 compared to the similar fraction of LynEGFP, which represents the membrane-associated fraction. The experiments raise the question whether the fast-migrating fraction is due to EGFP cleavage after Wnt3EGFP secretion. Although we cannot completely exclude some cleavage of EGFP from Wnt3, the fast diffusion coefficient in the brain ventricle ($53.62 \pm 13.69\ \mu m^2 s^{-1}$) is still significantly slower than that of secEGFP in the same location ($125.82 \pm 8.85\ \mu m^2 s^{-1}$), and thus represents at least partly intact Wnt3EGFP, possibly as small oligomers or a mixture of monomers and oligomers. These results are in line with different migration of cytosolic and membrane-bound versions of FPs detected previously (Shi et al., 2009).

Of particular interest are the elusive secreted fractions of Wnt, including the very slow-migrating fraction of Wnt3EGFP detected in the brain ventricle. The existence of such a fraction and its high heterogeneity suggest either an aggregation of the lipid-modified Wnt3EGFP (Vyas et al., 2008) or formation of complexes between Wnt3 and some extracellular matrix components, such

as heparan sulphate proteoglycan [HSPG (Kleinschmit et al., 2010)], lipoprotein (Neumann et al., 2009; Mulligan et al., 2012), exosomes (Gross et al., 2012) or secreted frizzled-related proteins (Mii and Taira, 2009). A similar “very slow” fraction of another ligand - FGF8 was previously detected by FCS (Yu et al., 2009). This is not very surprising since the activity of FGFs and Wnts both depends on evolutionarily conserved interactions with HSPG (Superina et al., 2014).

The existence of secreted fractions has been supported by experiments with an inhibitor of Wnt secretion – C59 that changed Wnt3EGFP mobility at the membrane. It is known that the hydrophobicity of Wnt is reduced in the absence of Porc due to a block of Wnt palmitoylation (Zhai et al., 2004; Takada et al., 2006). In this situation proteins loose membrane affinity, which could cause increased mobility of Wnt3EGFP. Post-translational palmitoylation is necessary for Wnts to be recognized and transported by Wntless (Wls) from the Golgi to the plasma membrane (Coombs et al., 2010; Herr and Basler, 2012). Therefore, Porc inhibition causes intracellular accumulation of Wnt3EGFP and a reduction of the membrane-bound fraction. Consequently, the secreted Wnt3EGFP was barely detected in the brain ventricle. The faster diffusion of Wnt3EGFP on the membrane, after partial Porc inhibition, could be a result of a mixture of palmitoylated and non-palmitoylated Wnt3EGFP reaching the plasma membrane. In addition, literature has shown for some Wnt molecules that palmitoylation is necessary for raft localization (Zhai et al., 2004). The non-palmitoylated Wnt3EGFP could then reside in the more fluid disordered liquid phase leading to an increase in diffusion coefficient. The exact mechanism of the faster diffusion of membrane bound non-palmitoylated Wnt3EGFP will be the topic of a future study. The reduction of the membrane-bound Wnt fraction correlated with malformed brain patterning whose severity is proportional to the temporal onset of C59-mediated inhibition of Wnt secretion. Exposure during neural plate formation led to the loss of forebrain and

midbrain (Figure S9D) in C59-treated embryos. Later drug exposure resulted in decreased cerebellum (Figure 8C). These results support the hypothesis that Porc is a crucial component in Wnt3 secretion. Significant variation of both mobility (D_2) and distribution (F_2, Figure 5F) is consistent with the differential inhibitor intake by individual cells resulting in a variation of Wnt3 blocking between individual cells. However, the mobility of the fast-migrating component was not affected. This is probably because the transportation of Wnt3EGFP from ER to membrane is not blocked completely by the sub-threshold concentration of C59 used in FCS measurements.

On the other hand, the inability of IWR-1 to affect Wnt3EGFP expression and secretion was expected. Unlike C59 acting at the level of Wnt secretion this inhibitor affects Wnt signaling in target cells at the level of downstream events of Wnt signaling mediated by β-catenin (Chen et al., 2009; Lu et al., 2009). Hence Wnt3EGFP transgenics may not be ideal to assess efficacy of IWR-1 inhibitor. In this respect these transgenics complement those developed to analyze downstream effects of the Wnt signaling (Moro et al., 2012). Nevertheless, the results of IWR-1 treatment emphasize the specificity of C59 action and support the existence of a secreted Wnt3 fraction.

In conclusion, several zebrafish transgenics expressing different versions of fluorescent proteins, including those of Wnt3 were developed. These tools were used for *in vivo* FCS analysis of Wnt3 migration and distribution. The measurements are consistent with the existence of four fractions of Wnt3EGFP in the developing brain of zebrafish, which represent the bulk of this protein – the fast-migrating intracellular fraction (representing transport of expressed Wnt3 to and from the membrane) and slow-migrating membrane fraction as well as two relatively minor secreted fractions – the fast-migrating fraction, which may represent free Wnt3, and the very

slow-migrating fraction, which may represent Wnt3 complexes with various components of the extracellular matrix. Given a significant elongation of signaling glia during late neurulation (Korzh, 2014), which probably correlates with a change in the nucleo-cytoplasm ratio, it might be of interest to compare in future studies changes in developmental dynamics and distribution of these fractions of Wnt3EGFP prior to and immediately after this dramatic morphogenetic rearrangement. The different wnt3 transgenics will also be a useful resource for further target gene profiles analysis, a topic not addressed in this publication.

MATERIALS AND METHODS

Detailed Materials and Methods are provided in the supplement to this article.

ACKNOWLEDGEMENTS

C59 was kindly provided by Drs. May Ann Lee, Zhiyuan Ke and David Virshup. SGY was supported by an NUS scholarship. TW gratefully acknowledges funding by a grant from the Singapore Ministry of Education (MOE2012-T2-1-101, R-154-000-543-112). VK, HYS and CT are supported by Institute of Molecular and Cell Biology institutional grant from the Agency for Science, Technology, and Research (A*STAR) of Singapore. VK and CT are also supported by A*STAR Nutrition and Food Science grant (1121770041).

Author Contribution: CT designed and generated the *wnt3* promoter-driven transgenic lines, conducted *in vivo* analysis of *wnt3* transgenics and wrote the paper; SGY designed and

performed the FCS experiments, analyzed the data and wrote the paper; HYS made the recombinant CMV-Wnt3EGFP construct and validated its activity in zebrafish; VK and TW designed the experiments, supervised the work, wrote and approved the paper.

CONFLICT OF INTEREST

The authors declare that they have no conflict of interest.

References

Anastas, J. N. and Moon, R. T. (2013) 'WNT signalling pathways as therapeutic targets in cancer', *Nature Reviews Cancer* 13(1): 11-26.

Anne, S. L., Govek, E. E., Ayrault, O., Kim, J. H., Zhu, X., Murphy, D. A., Van Aelst, L., Roussel, M. F. and Hatten, M. E. (2013) 'WNT3 inhibits cerebellar granule neuron progenitor proliferation and medulloblastoma formation via MAPK activation', *Plos One* 8(11): e81769.

Balciunas, D., Wangensteen, K. J., Wilber, A., Bell, J., Geurts, A., Sivasubbu, S., Wang, X., Hackett, P. B., Largaespada, D. A., McIvor, R. S. et al. (2006) 'Harnessing a high cargo-capacity transposon for genetic applications in vertebrates', *Plos Genetics* 2(11): 1715-1724.

Blader, P., Strahle, U. and Ingham, P. W. (1996) 'Three Wnt genes expressed in a wide variety of tissues during development of the zebrafish, Danio rerio: developmental and evolutionary perspectives', *Development genes and evolution* 206(1): 3-13.

Bonner, J., Gribble, S. L., Veien, E. S., Nikolaus, O. B., Weidinger, G. and Dorsky, R. I. (2008) 'Proliferation and patterning are mediated independently in the dorsal spinal cord downstream of canonical Wnt signaling', *Developmental biology* 313(1): 398-407.

Bulfone, A., Puelles, L., Porteus, M. H., Frohman, M. A., Martin, G. R. and Rubenstein, J. L. (1993) 'Spatially restricted expression of Dlx-1, Dlx-2 (Tes-1), Gbx-2, and Wnt-3 in the embryonic day 12.5 mouse forebrain defines potential transverse and longitudinal segmental boundaries', *The Journal of neuroscience : the official journal of the Society for Neuroscience* 13(7): 3155-72.

Chen, B. Z., Dodge, M. E., Tang, W., Lu, J. M., Ma, Z. Q., Fan, C. W., Wei, S. G., Hao, W. N., Kilgore, J., Williams, N. S. et al. (2009) 'Small molecule-mediated disruption of Wnt-dependent signaling in tissue regeneration and cancer', *Nature Chemical Biology* 5(2): 100-107.

Clements, W. K., Ong, K. G. and Traver, D. (2009) 'Zebrafish wnt3 Is Expressed in Developing Neural Tissue', *Developmental Dynamics* 238(7): 1788-1795.

Clevers, H. and Nusse, R. (2012) 'Wnt/beta-Catenin Signaling and Disease', *Cell* 149(6): 1192-1205.

Coombs, G. S., Yu, J., Canning, C. A., Veltri, C. A., Covey, T. M., Cheong, J. K., Utomo, V., Banerjee, N., Zhang, Z. H., Jadulco, R. C. et al. (2010) 'WLS-dependent secretion of WNT3A requires Ser209 acylation and vacuolar acidification', *Journal of Cell Science* 123(19): 3357-3367.

Dorsky, R. I., Sheldahl, L. C. and Moon, R. T. (2002) 'A transgenic Lef1/beta-catenin-dependent reporter is expressed in spatially restricted domains throughout zebrafish development', *Developmental biology* 241(2): 229-37.

Foo, Y. H., Korzh, V. and Wohland, T. (2012) 'Fluorescence Correlation and Cross-Correlation Spectroscopy Using Fluorescent Proteins for Measurements of Biomolecular Processes in Living Organisms', *Fluorescent Proteins II Springer Series on Fluorescence* 12: 213-248.

493 Garriock, R. J., Warkman, A. S., Meadows, S. M., D'Agostino, S. and Krieg, P. A. (2007)
494 'Census of vertebrate Wnt genes: isolation and developmental expression of
495 Xenopus Wnt2, Wnt3, Wnt9a, Wnt9b, Wnt10a, and Wnt16', *Developmental*
496 *dynamics : an official publication of the American Association of Anatomists* 236(5):
497 1249-58.
498 Gross, J. C., Chaudhary, V., Bartscherer, K. and Boutros, M. (2012) 'Active Wnt
499 proteins are secreted on exosomes', *Nature Cell Biology* 14(10): 1036–1045.
500 Guo, S. M., He, J., Monnier, N., Sun, G. Y., Wohland, T. and Bathe, M. (2012)
501 'Bayesian Approach to the Analysis of Fluorescence Correlation Spectroscopy Data
502 II: Application to Simulated and In Vitro Data', *Analytical Chemistry* 84(9): 3880-3888.
503 Hashimoto, M. and Hibi, M. (2012) 'Development and evolution of cerebellar neural
504 circuits', *Development Growth & Differentiation* 54(3): 373-389.
505 Herr, P. and Basler, K. (2012) 'Porcupine-mediated lipidation is required for Wnt
506 recognition by Wls', *Developmental biology* 361(2): 392-402.
507 Jessell, T. M. (2000) 'Neuronal specification in the spinal cord: Inductive signals and
508 transcriptional codes', *Nature Reviews Genetics* 1(1): 20-29.
509 Kaslin, J., Kroehne, V., Benato, F., Argenton, F. and Brand, M. (2013) 'Development
510 and specification of cerebellar stem and progenitor cells in zebrafish: from embryo to
511 adult', *Neural development* 8: 9.
512 Kim, M., Lee, H. C., Tsedensodnom, O., Hartley, R., Lim, Y. S., Yu, E., Merle, P. and
513 Wands, J. R. (2008) 'Functional interaction between Wnt3 and Frizzled-7 leads to
514 activation of the Wnt/beta-catenin signaling pathway in hepatocellular carcinoma
515 cells', *Journal of hepatology* 48(5): 780-91.
516 Kleinschmit, A., Koyama, T., Dejima, K., Hayashi, Y., Kamimura, K. and Nakato, H.
517 (2010) 'Drosophila heparan sulfate 6-O endosulfatase regulates Wingless
518 morphogen gradient formation', *Developmental biology* 345(2): 204-14.
519 Kobune, M., Chiba, H., Kato, J., Kato, K., Nakamura, K., Kawano, Y., Takada, K.,
520 Takimoto, R., Takayama, T., Hamada, H. et al. (2007) 'Wnt3/RhoA/ROCK signaling
521 pathway is involved in adhesion-mediated drug resistance of multiple myeloma in an
522 autocrine mechanism', *Molecular cancer therapeutics* 6(6): 1774-84.
523 Kondrychyn, I., Teh, C., Garcia-Lecea, M., Guan, Y. X., Kang, A. and Korzh, V. (2011)
524 'Zebrafish Enhancer TRAP Transgenic Line Database ZETRAP 2.0', *Zebrafish* 8(4):
525 181-182.
526 Kondrychyn, I., Teh, C., Sin, M. and Korzh, V. (2013) 'Stretching morphogenesis of the
527 roof plate and formation of the central canal', *Plos One* 8(2): e56219.
528 Korzh, V. (2014) 'Stretching cell morphogenesis during late neurulation and mild neural
529 tube defects', *Development, Growth & Differentiation* 56(6): 425–433.
530 Korzh, V., Kondrichin, I. and García-Lecea, M. (2007) 'Gliogenesis in zebrafish', *In:*
531 *Trends in Glial Research-Basic and Applied. Eds: S.T. Dheen and E.A. Ling,*
532 *Research Signpost*: 81-98.
533 Krauss, S., Korzh, V., Fjose, A. and Johansen, T. (1992) 'Expression of four zebrafish
534 wnt-related genes during embryogenesis', *Development* 116(1): 249-59.

Lancaster, M. A., Gopal, D. J., Kim, J., Saleem, S. N., Silhavy, J. L., Louie, C. M., Thacker, B. E., Williams, Y., Zaki, M. S. and Gleeson, J. G. (2011) 'Defective Wnt-dependent cerebellar midline fusion in a mouse model of Joubert syndrome', *Nature medicine* 17(6): 726-31.

Liu, P. T., Wakamiya, M., Shea, M. J., Albrecht, U., Behringer, R. R. and Bradley, A. (1999) 'Requirement for Wnt3 in vertebrate axis formation', *Nature Genetics* 22(4): 361-365.

Lu, J. M., Ma, Z. Q., Hsieh, J. C., Fan, C. W., Chen, B. Z., Longgood, J. C., Williams, N. S., Amatruda, J. F., Lum, L. and Chen, C. (2009) 'Structure-activity relationship studies of small-molecule inhibitors of Wnt response', *Bioorganic & Medicinal Chemistry Letters* 19(14): 3825-3827.

Machan, R. and Wohland, T. (2014) 'Recent applications of fluorescence correlation spectroscopy in live systems', *FEBS Letters* 588(19): 3571-84.

Mii, Y. and Taira, M. (2009) 'Secreted Frizzled-related proteins enhance the diffusion of Wnt ligands and expand their signalling range', *Development* 136(24): 4083-4088.

Millen, K. J., Hui, C. C. and Joyner, A. L. (1995) 'A role for En-2 and other murine homologues of Drosophila segment polarity genes in regulating positional information in the developing cerebellum', *Development* 121(12): 3935-45.

Molven, A., Njolstad, P. R. and Fjose, A. (1991) 'Genomic structure and restricted neural expression of the zebrafish wnt-1 (int-1) gene', *The EMBO journal* 10(4): 799-807.

Moro, E., Ozhan-Kizil, G., Mongera, A., Beis, D., Wierzbicki, C., Young, R. M., Bournele, D., Domenichini, A., Valdivia, L. E., Lum, L. et al. (2012) 'In vivo Wnt signaling tracing through a transgenic biosensor fish reveals novel activity domains', *Developmental biology* 366(2): 327-40.

Muller, P., Rogers, K. W., Yu, S. R., Brand, M. and Schier, A. F. (2013) 'Morphogen transport', *Development* 140(8): 1621-38.

Mulligan, K. A., Fuerer, C., Ching, W., Fish, M., Willert, K. and Nusse, R. (2012) 'Secreted Wingless-interacting molecule (Swim) promotes long-range signaling by maintaining Wingless solubility', *Proceedings of the National Academy of Sciences of the United States of America* 109(2): 370-377.

Mütze, J., Ohrt, T. and Schwille, P. (2011) 'Fluorescence correlation spectroscopy in vivo', *Laser & Photonics Reviews* 5(1): 52-67.

Neumann, S., Coudreuse, D. Y. M., van der Westhuyzen, D. R., Eckhardt, E. R. M., Korswagen, H. C., Schmitz, G. and Sprong, H. (2009) 'Mammalian Wnt3a is Released on Lipoprotein Particles', *Traffic* 10(3): 334-343.

Niemann, S., Zhao, C. F., Pascu, F., Stahl, U., Aulepp, U., Niswander, L., Weber, J. L. and Muller, U. (2004) 'Homozygous WNT3 mutation causes tetra-amelia in a large consanguineous family', *American Journal of Human Genetics* 74(3): 558-563.

Nusse, R. and Varmus, H. (2012) 'Three decades of Wnts: a personal perspective on how a scientific field developed', *The EMBO journal* 31(12): 2670-84.

Nusse, R. and Varmus, H. E. (1982) 'Many tumors induced by the mouse mammary tumor virus contain a provirus integrated in the same region of the host genome', *Cell* 31(1): 99-109.

Pan, X. T., Foo, W., Lim, W., Fok, M. H. Y., Liu, P., Yu, H., Maruyama, I. and Wohland, T. (2007a) 'Multifunctional fluorescence correlation microscope for intracellular and microfluidic measurements', *Review of Scientific Instruments* 78(5).

Pan, X. T., Yu, H., Shi, X. K., Korzh, V. and Wohland, T. (2007b) 'Characterization of flow direction in microchannels and zebrafish blood vessels by scanning fluorescence correlation spectroscopy', *Journal of Biomedical Optics* 12(1).

Park, H. C., Kim, C. H., Bae, Y. K., Yeo, S. Y., Kim, S. H., Hong, S. K., Shin, J., Yoo, K. W., Hibi, M., Hirano, T. et al. (2000) 'Analysis of upstream elements in the HuC promoter leads to the establishment of transgenic zebrafish with fluorescent neurons', *Developmental biology* 227(2): 279-93.

Proffitt, K. D., Madan, B., Ke, Z. Y., Pendharkar, V., Ding, L. J., Lee, M. A., Hannoush, R. N. and Virshup, D. M. (2013) 'Pharmacological Inhibition of the Wnt Acyltransferase PORCN Prevents Growth of WNT-Driven Mammary Cancer', *Cancer Research* 73(2): 502-507.

Ries, J., Yu, S. R., Burkhardt, M., Brand, M. and Schwille, P. (2009) 'Modular scanning FCS quantifies receptor-ligand interactions in living multicellular organisms', *Nature Methods* 6(9): 643-U31.

Robu, M. E., Larson, J. D., Nasevicius, A., Beiraghi, S., Brenner, C., Farber, S. A. and Ekker, S. C. (2007) 'p53 activation by knockdown technologies', *Plos Genetics* 3(5): e78.

Roelink, H. and Nusse, R. (1991) 'Expression of two members of the Wnt family during mouse development--restricted temporal and spatial patterns in the developing neural tube', *Genes & development* 5(3): 381-8.

Selvadurai, H. J. and Mason, J. O. (2011) 'Wnt/beta-catenin signalling is active in a highly dynamic pattern during development of the mouse cerebellum', *Plos One* 6(8): e23012.

Shi, X. K., Teo, L. S., Pan, X. T., Chong, S. W., Kraut, R., Korzh, V. and Wohland, T. (2009) 'Probing Events with Single Molecule Sensitivity in Zebrafish and Drosophila Embryos by Fluorescence Correlation Spectroscopy', *Developmental Dynamics* 238(12): 3156-3167.

Stanganello, E., Hagemann, A. I., Mattes, B., Sinner, C., Meyen, D., Weber, S., Schug, A., Raz, E. and Scholpp, S. (2015) 'Filopodia-based Wnt transport during vertebrate tissue patterning', *Nature communications* 6: 5846.

Stewart, S., Gomez, A. W., Armstrong, B. E., Henner, A. and Stankunas, K. (2014) 'Sequential and Opposing Activities of Wnt and BMP Coordinate Zebrafish Bone Regeneration', *Cell Reports* 6(3): 482-498.

Sun, G., Guo, S. M., Teh, C., Korzh, V., Bathe, M. and Wohland, T. (2015) 'Bayesian model selection applied to the analysis of fluorescence correlation spectroscopy data of fluorescent proteins in vitro and in vivo', *Analytical Chemistry* 87(8): 4326-33.

Superina, S., Borovina, A. and Ciruna, B. (2014) 'Analysis of maternal-zygotic ugdh mutants reveals divergent roles for HSPGs in vertebrate embryogenesis and

provides new insight into the initiation of left-right asymmetry', *Developmental biology* 387(2): 154-66.

Takada, R., Satomi, Y., Kurata, T., Ueno, N., Norioka, S., Kondoh, H., Takao, T. and Takada, S. (2006) 'Monounsaturated fatty acid modification of Wnt protein: Its role in Wnt secretion', *Developmental Cell* 11(6): 791-801.

Tanaka, K., Okabayashi, K., Asashima, M., Perrimon, N. and Kadowaki, T. (2000) 'The evolutionarily conserved porcupine gene family is involved in the processing of the Wnt family', *European Journal of Biochemistry* 267(13): 4300-4311.

van de Water, S., van de Wetering, M., Joore, J., Esseling, J., Bink, R., Clevers, H. and Zivkovic, D. (2001) 'Ectopic Wnt signal determines the eyeless phenotype of zebrafish masterblind mutant', *Development* 128(20): 3877-88.

Vyas, N., Goswami, D., Manonmani, A., Sharma, P., Ranganath, H. A., VijayRaghavan, K., Shashidhara, L. S., Sowdhamini, R. and Mayor, S. (2008) 'Nanoscale organization of Hedgehog is essential for long-range signaling', *Cell* 133(7): 1214-1227.

Willert, K., Brown, J. D., Danenberg, E., Duncan, A. W., Weissman, I. L., Reya, T., Yates, J. R. and Nusse, R. (2003) 'Wnt proteins are lipid-modified and can act as stem cell growth factors', *Nature* 423(6938): 448-452.

Ye, W. L., Bouchard, M., Stone, D., Liu, X. D., Vella, F., Lee, J., Nakamura, H., Ang, S. L., Busslinger, M. and Rosenthal, A. (2001) 'Distinct regulators control the expression of the mid-hindbrain organizer signal FGF8', *Nature Neuroscience* 4(12): 1175-1181.

Ye, W. L., Shimamura, K., Rubenstein, J. L. R., Hynes, M. A. and Rosenthal, A. (1998) 'FGF and Shh signals control dopaminergic and serotonergic cell fate in the anterior neural plate', *Cell* 93(5): 755-766.

Yin, A., Korzh, V. and Gong, Z. Y. (2012) 'Perturbation of zebrafish swimbladder development by enhancing Wnt signaling in Wif1 morphants', *Biochimica Et Biophysica Acta-Molecular Cell Research* 1823(2): 236-244.

Yu, S. R., Burkhardt, M., Nowak, M., Ries, J., Petrasek, Z., Scholpp, S., Schwille, P. and Brand, M. (2009) 'Fgf8 morphogen gradient forms by a source-sink mechanism with freely diffusing molecules', *Nature* 461(7263): 533-U100.

Zhai, L., Chaturvedi, D. and Cumberledge, S. (2004) 'Drosophila Wnt-1 undergoes a hydrophobic modification and is targeted to lipid rafts, a process that requires porcupine', *Journal of Biological Chemistry* 279(32): 33220-33227.

Zhou, S. H., Lo, W. C., Suhalim, J. L., Digman, M. A., Gratton, E., Nie, Q. and Lander, A. D. (2012) 'Free Extracellular Diffusion Creates the Dpp Morphogen Gradient of the Drosophila Wing Disc', *Current Biology* 22(8): 668-675.

Figure Legends

Figure 1 – EGFP and Wnt3 expression in transgenics under control of the *wnt3* promoter. A stable zebrafish transgenic line containing the 4 kb *wnt3* promoter drives EGFP expression in a *wnt3*-like manner with spatio-temporal correlation with endogenous transcripts. (**A**) *egfp* transcripts expression (magenta) in 4kb *wnt3* promoter transgenic line Tg(-4.0*wnt3*:EGFP)^{F1} colocalized with *ptc1* (pink) at the zli at 24 hpf. (**B**) An *in vivo* image of 24 hpf Tg(-4.0*wnt3*:EGFP)^{F1} showing EGFP (+) domains highlighted by the transgenic line. (**C,E**) *wnt3* transcripts are detected in the cerebellum (ce), epithalamus (ep), floor plate (fp), optic tectum (ot), roof plate (rp), midbrain hindbrain boundary (mhb) and hindbrain (hb) of 48hpf (C) and 72hpf (E) larvae. (**D,F**) *in vivo* images of Tg(-4.0*wnt3*:EGFP)^{F1} at 48hpf (E) and 72hpf (G) showing similar EGFP(+) domains. (**G-J**) Comparison of midbrain (G-H) and cerebellum (I-J) cross sections of *wnt3* expression in a 48hpf zebrafish brain with corresponding cross sections of Tg(-4.0*wnt3*:EGFP)^{F1} that detected EGFP expression in similar regions. *wnt3*-positive domains include the (ot), (fp), and (ce). (H', H''and J) Co-immunohistochemical detection of EGFP and Hu-positive neurons showed that EGFP (+) domains in the (rp), (fp) and (ce) are flanked by neurons. A 100 mm scale bar is shown in each image.

Abbreviations: ce - cerebellum, ep - epithalamus, fp - floor plate, ot - optic tectum, rp - roof plate, mhb - midbrain hindbrain boundary and hb – hindbrain.

Figure 2 – Spatio-temporal expression of *wnt3* promoter-driven EGFP/Wnt3EGFP. Spatio-temporal expression of 4kb *wnt3* promoter-driven EGFP/Wnt3EGFP influenced by genomic insertion of a transgene vary in strength . Tg(-4.0*wnt3*: EGFP)^{F1}, Tg(-4.0*wnt3*:Wnt3EGFP)^{F1},

683 Tg(-4.0*wnt3*:Wnt3EGFP)^{F2} and Tg(-4.0*wnt3*:Wnt3EGFP)^{F3} are abbreviated in the figure as
684 Tg(*wnt3*:EGFP)^{F1}, Tg(*wnt3*:Wnt3EGFP)^{F1}, Tg(*wnt3*:Wnt3EGFP)^{F2} and Tg(*wnt3*:Wnt3EGFP)^{F3},
685 respectively. (**A-O**) Initial spatio-temporal similarity of expression of EGFP and Wnt3EGFP is
686 maintained in three independent transgenic lines. (**P-W**) Tg(-4.0*wnt3*:Wnt3EGFP)^{F3} maintains
687 strong Wnt3EGFP expression in the cerebellum beyond 48 hpf. Transgene expression in the
688 optic tectum and cerebellum decreases from 48 hpf in all other Wnt3 transgenics. Abbreviations:
689 ce – cerebellum, ot - optic tectum.

690

691 **Figure 3 – The size of MHB and cerebellum segmental volume correlates with the level of**
692 **Wnt3EGFP expression.** (A-C) *In vivo* comparison of segmental volume in Tg(memKR15-16) at
693 the EGFP or different Wnt3EGFP transgenics background at 4 dpf. Tg(memKR15-16)/EGFP (A),
694 Tg(memKR15-16)/Wnt3EGFP [Tg(*wnt3*:Wnt3EGFP)^{F2}] (B) and Tg(memKR15-16)/ Wnt3EGFP
695 in Tg(*wnt3*:Wnt3EGFP)^{F3} (C). (D) The increase in segmental volume in Tg(memKR15-16) is
696 significant according to unpaired t-test comparing Tg(*wnt3*:EGFP)^{F1} vs Tg(*wnt3*:wnt3EGFP)^{F3}
697 (P=0.0022).

698

699 **Figure 4 –Expression of Wnt3EGFP in the cerebellum of Tg(*wnt3*:Wnt3EGFP)^{F3} partially**
700 **compensates cerebellum growth in MO1 injected Wnt3 morphants.** (A-D) Dorsal view of
701 double transgenic larvae Tg(memKR15-16) co-expressing KillerRed with EGFP from
702 Tg(*wnt3*:EGFP)^{F1} (A-B) or Wnt3EGFP from Tg(*wnt3*:Wnt3EGFP)^{F3}(C-D). KillerRed is
703 expressed in the MHB and cerebellum. Reduction in KR-positive cerebellum is partially
704 compensated in 3dpf Tg(*wnt3*:Wnt3EGFP)^{F3} MO1-morphants (D). (E-H) 3D lateral view of
705 KR-positive MHB and cerebellum in Tg(*wnt3*:EGFP)^{F1} (E), MO1-injected Tg(*wnt3*:EGFP)^{F1} (F),

706 Tg (*wnt3*:Wnt3EGFP)^{F3} (G) and MO1-injected Tg (*wnt3*:Wnt3EGFP)^{F3} at 3dpf (H). (I) Scatter
707 plot of computed volume. The decrease in segmental volume in Tg(memKR15-16) is significant
708 between MO1-morphants and un-injected siblings. Unpaired t-test comparing Tg(*wnt3*:EGFP)^{F1}
709 vs MO1-morphant Tg(*wnt3*:EGFP)^{F1} (P<0.0001); Tg(*wnt3*:wnt3EGFP)^{F3} vs MO1-morphants
710 Tg(*wnt3*:Wnt3EGFP)^{F3} (P=0.0034). Segmental volume in MO1-morphant
711 Tg(*wnt3*:Wnt3EGFP)^{F3} remains significantly higher than in MO1-morphant Tg(*wnt3*:EGFP)^{F1}
712 (P=0.0003).
713
714 **Figure 5 – FCS analysis of Wnt3EGFP and LynEGFP membrane dynamics in the**
715 **cerebellum.** (**A**) Autocorrelation curve of Wnt3EGFP on the plasma membrane. The curve is
716 fitted into a two-component model including a blinking process. Dotted line represents the
717 experimental data. Solid line is the fit curve. (**B, C**) Diffusion coefficients (D_1, D_2) extracted
718 from fit at different development stages. (**D**) Fraction of slow-migrating component (F_2)
719 extracted from fit at different developmental stages. The difference in membrane fraction of
720 LynEGFP and Wnt3EGFP indicates the existence of a small amount of intercellular Wnt3EGFP.
721 Data are mean ± SD. Red bar, Wnt3EGFP. Green bar, LynEGFP. Significance level, two-way t-
722 test, *P < 0.001. See also Figure S1 and Table S1.
723
724 **Figure 6 – Wnt3EGFP, LynEGFP and secEGFP in 4th brain ventricle.** (**A**) Confocal image
725 of zebrafish cerebellum expressing Wnt3EGFP at 34 hpf. Scale bar, 50 μm. (**B**) Three times
726 zoom in of (A) with focus on the cerebellum boundary and flanking brain ventricle. Scale bar, 20
727 μm. Images were taken in dorsal view. Ce: cerebellum; BV: brain ventricle. The images were
728 modified using Imaris to increase the contrast. (**C**) Normalized intensity from the cerebellum

boundary cell to the brain ventricle along the white arrow in (B) of Wnt3EGFP (red), LynEGFP (green) and secEGFP (blue). Data are the average of three scannings of three embryos for each type. (**D**) Normalized ACF curves taken in position within a ventricle at 100 μm from the cerebellum boundary. Color-coding is the same as in B together with wild type (WT, dotted grey). The results show the free diffusion of Wnt3EGFP and secEGFP in the brain ventricle, whereas no fluorescence can be detected neither for LynEGFP nor for WT. (**E**) Diffusion coefficients extracted from fit for different types of EGFP-labeled proteins in both the cerebellum and the brain ventricle. secEGFP serves as an intercellular indicator of protein mobility in multicellular tissue and extracellular indicator in the brain ventricle. EGFP reporter Tg(-4.0*wnt3*:EGFP)^{F2} and LynEGFP transgenics Tg(*-8.0cldnB:*lynEGFP) serve as an indicator of intracellular protein mobility. Data are mean ± SD. Light grey bar, BV. Dark grey bar, ce. See also Figure S2 and Table S2, S3.

Abbreviations - Ce: cerebellum; BV: brain ventricle.

Figure 7 – Wnt3EGFP secretion is affected by the block of Porcupine. (**A**, **B**) Confocal images of zebrafish cerebellum expressing Wnt3EGFP and LynEGFP after C59 treatment. The embryos were treated with 5 μM C59 10 - 28 hpf (for details, see M&M). The samples were briefly soaked in 1x egg water before imaging in dorsal view and FCS measurement. Scale bar, 50 μm. (**C**, **D** and **E**) Diffusion coefficients (D_1, D_2) and protein membrane distribution (F_2) extracted from fit at different conditions for both Wnt3EGFP and LynEGFP. (F) The results show that FCS signatures remain unchanged for LynEGFP, indicating that properties of plasma membrane are not influenced by treatment or the drug function. Data are mean ± SD. Red bar,

Wnt3EGFP. Green bar, LynEGFP. Significance level, two-way t-test, *P < 0.001. See also Table S3.

Figure 8 – Exposure of Tg(*wnt3*:Wnt3EGFP)^{F3} larvae to Wnt inhibitor C59 decreased the segmental volume of cerebellum in Tg(memKR15-16). (**A-D**) *In vivo* images of 3 dpf double transgenic larvae: control Tg(*wnt3*:EGFP)^{F1}/Tg(memKR15-16) (**A**), Tg(*wnt3*:Wnt3EGFP)^{F3}/Tg(memKR15-16) (**B-D**). All Tg(*wnt3*:wnt3EGFP)^{F3} double transgenic larvae were exposed to 1% DMSO (**B**), 5µm C59 (**C**) or 50 µM IWR-1 (**D**) at 36 hpf-stage for 36 hours before assaying expression of fluorescent reporter at 72 hpf. High-magnification view of representative EGFP/Wnt3EGFP-expressing cells from different treatment groups (insets). (**E**) A bar chart comparing the resultant KillerRed-positive brain segment in Tg(memKR15-16). Significant decrease was observed where unpaired t-test compared segmental volumes in 1%DMSO-treated Tg(*wnt3*:Wnt3EGFP)^{F3} vs C59-treated Tg(*wnt3*:Wnt3EGFP)^{F3} (P=0.0001).

Figure 9 – Four fractions of Wnt3EGFP in the cerebellum and brain ventricle. (**A**) Schematic of Wnt3EGFP fractions: two intracellular fractions: i) a fast-migrating intracellular fraction, ii) slow-migrating membrane fraction; and two secreted fractions: iii) a fast-migrating diffusing fraction and, iv) a very slow-migrating one. (**B**) C59-treated Wnt3EGFP with reduced membrane-bound and secreted Wnt3EGFP. Ce: cerebellum; BV: brain ventricle.

Abbreviations: Ce: cerebellum; BV: brain ventricle.

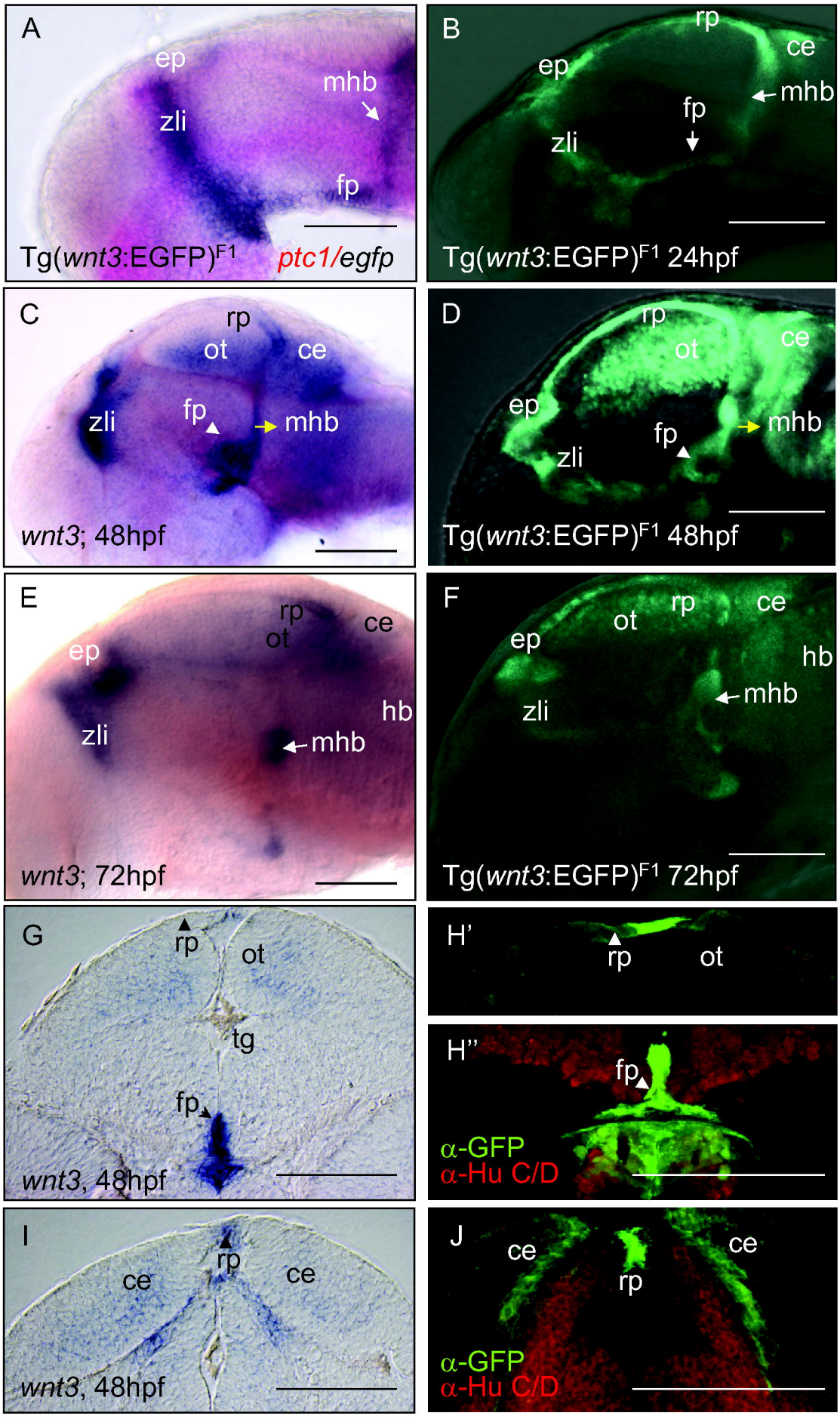

Fig. 1 - Teh et al.

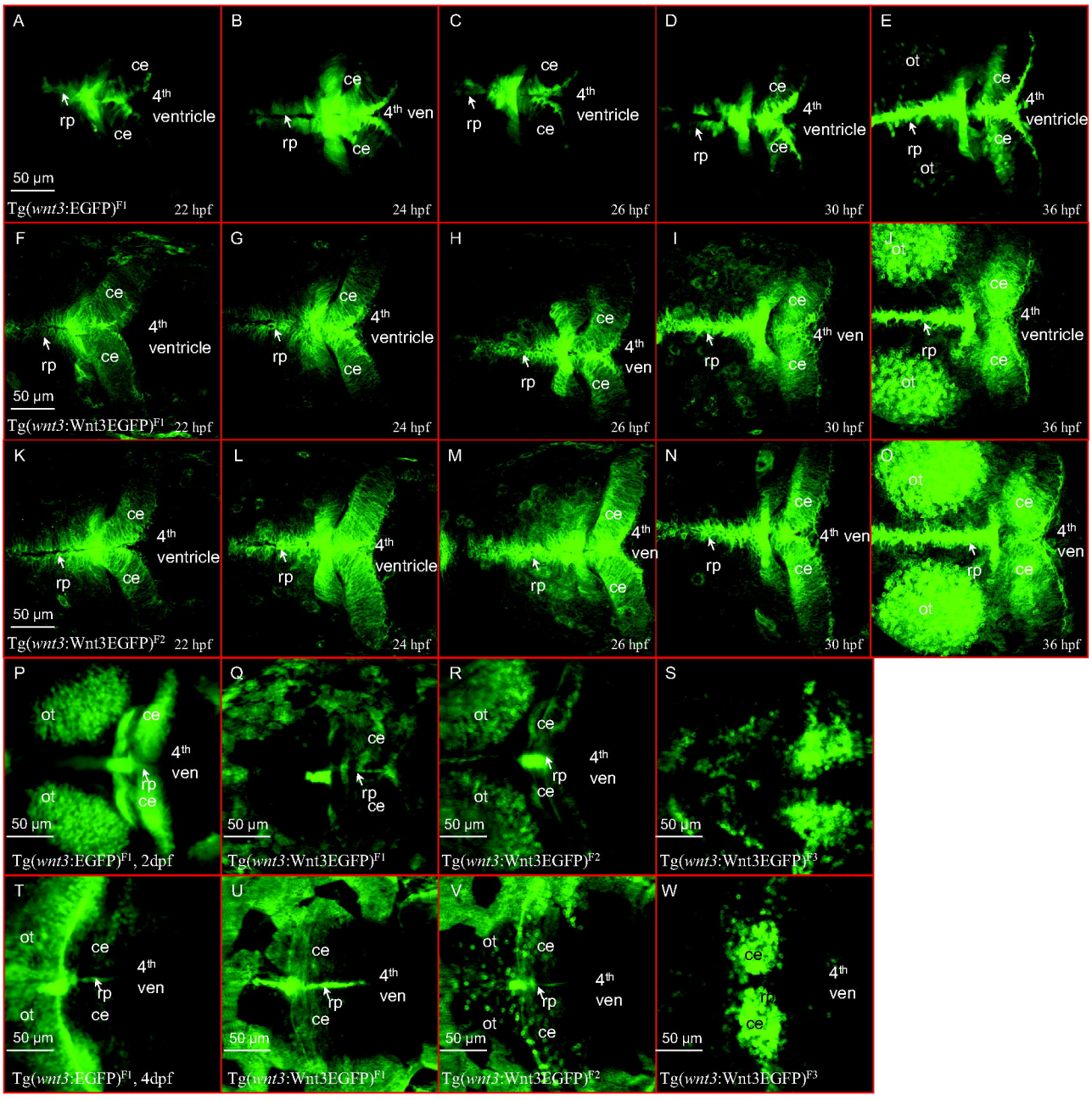

Fig. 2 - Teh et al.

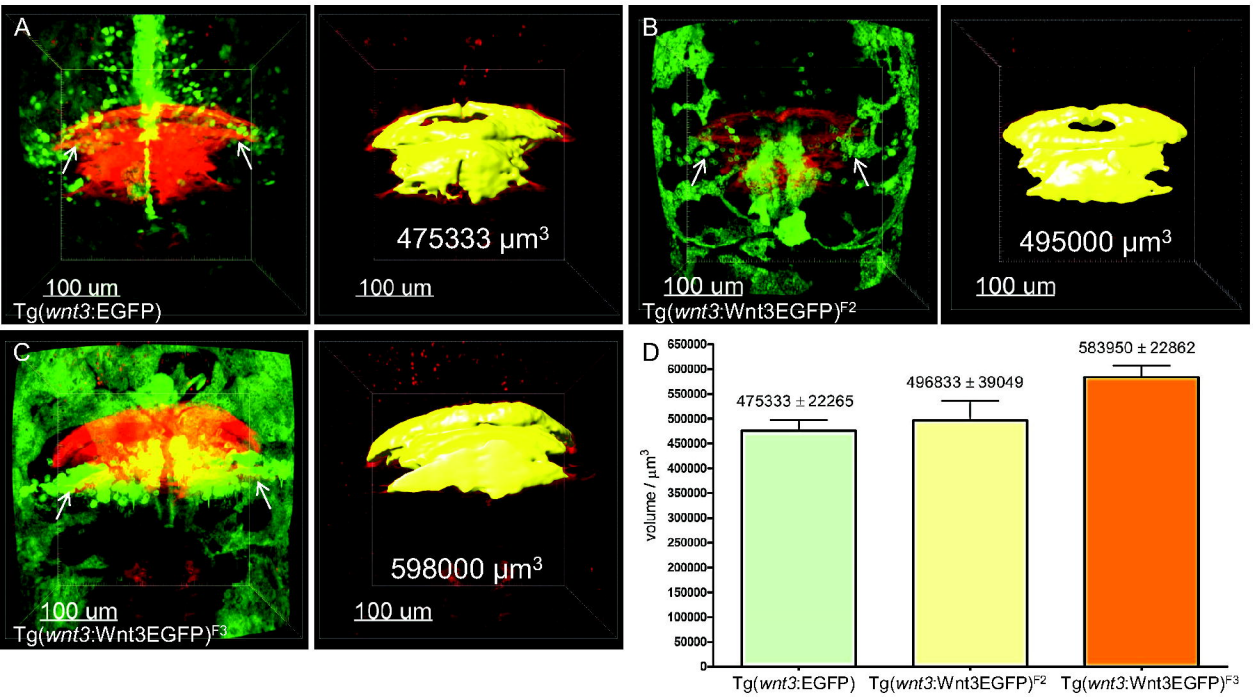

Fig. 3 - Teh et al.

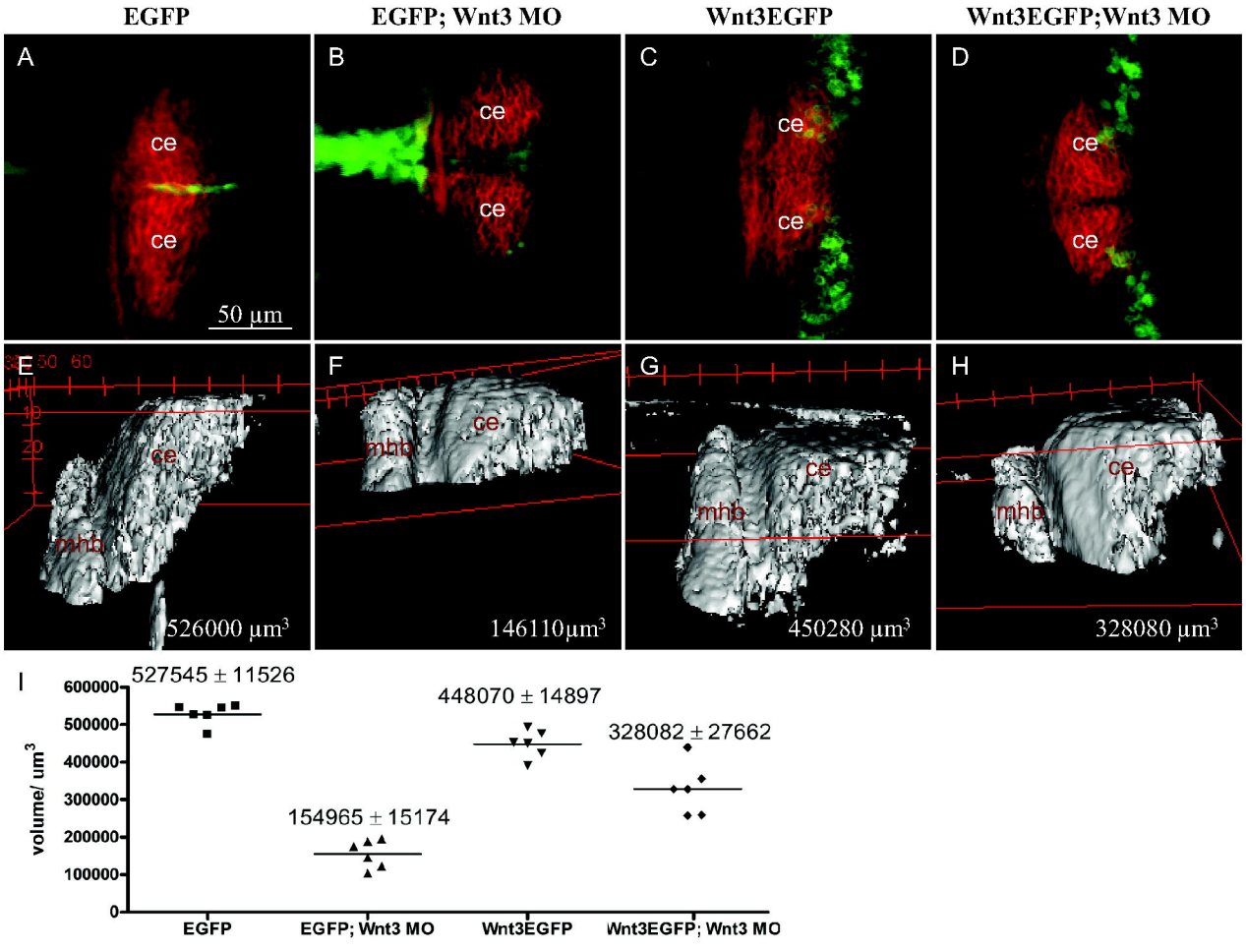

Fig. 4 - Teh et al.

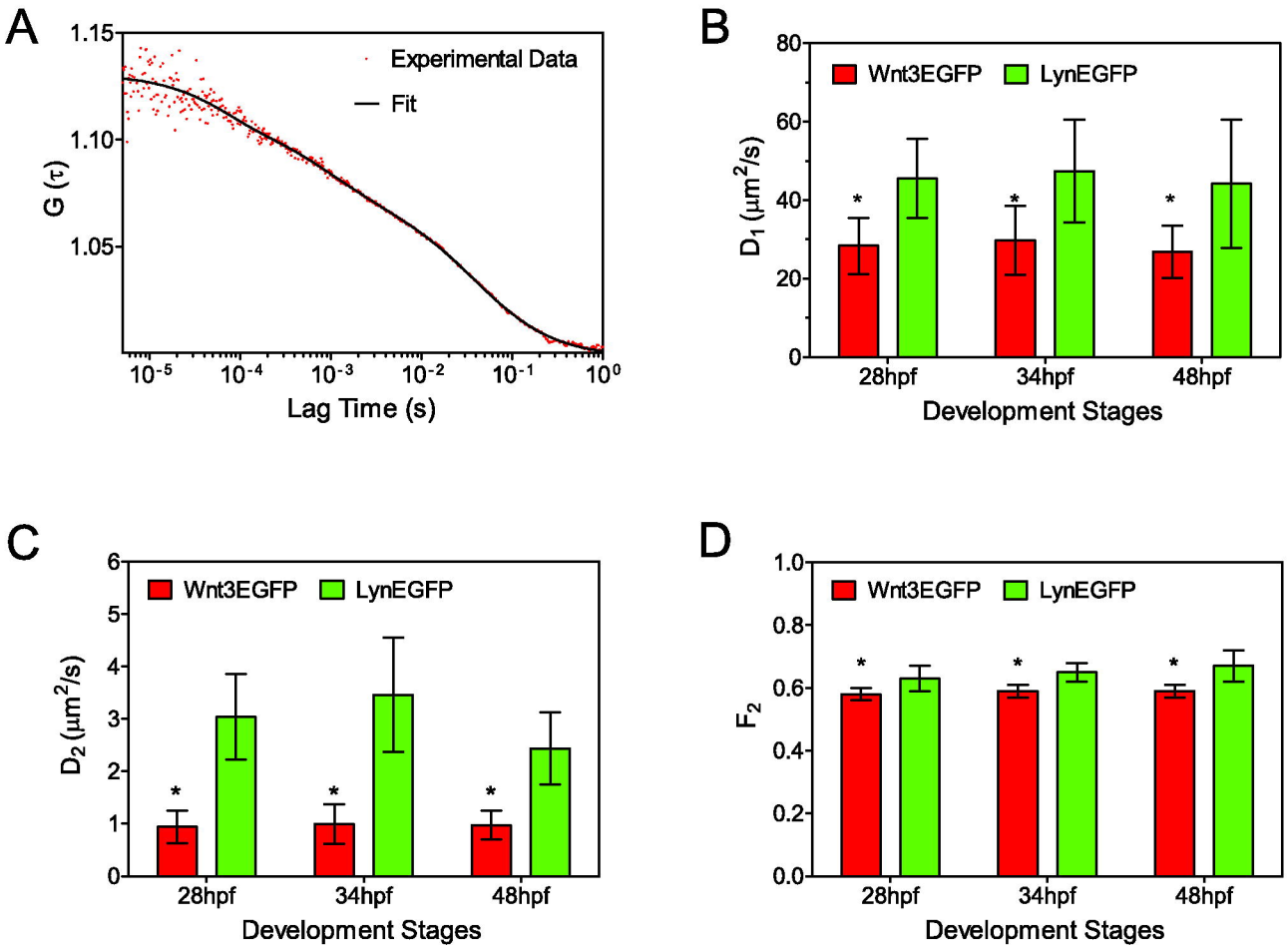

Fig. 5 - Teh et al.

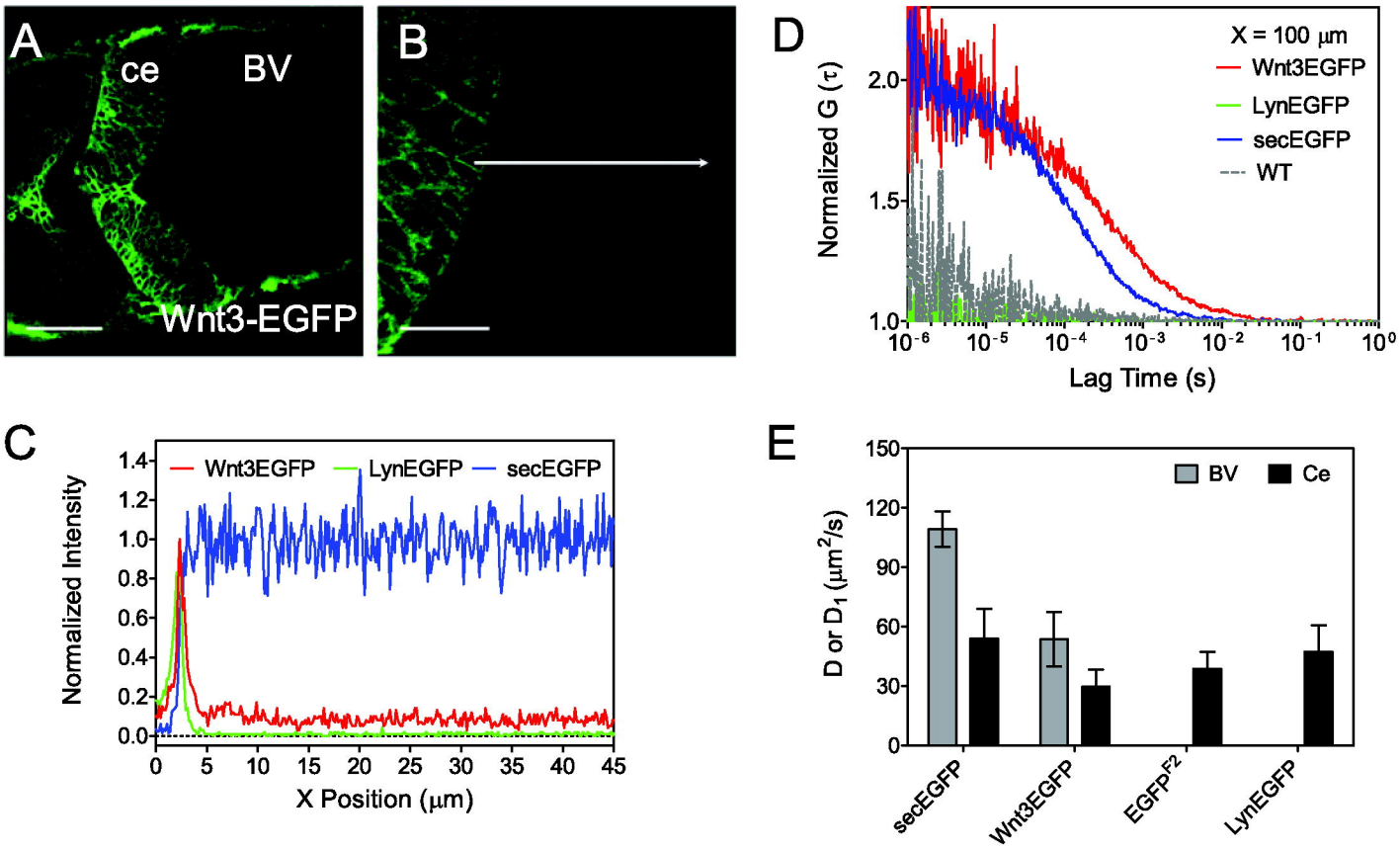

Fig. 6 - Teh et al.

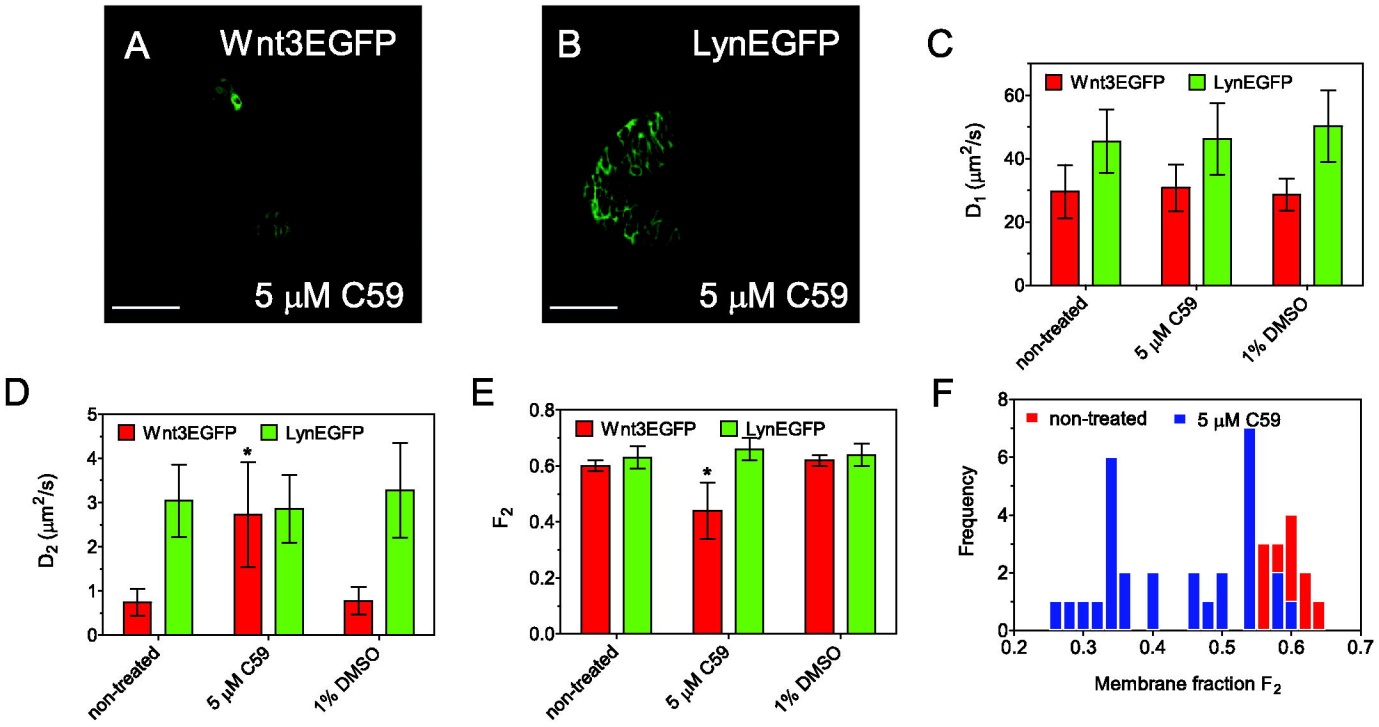

Fig. 7 - Teh et al.

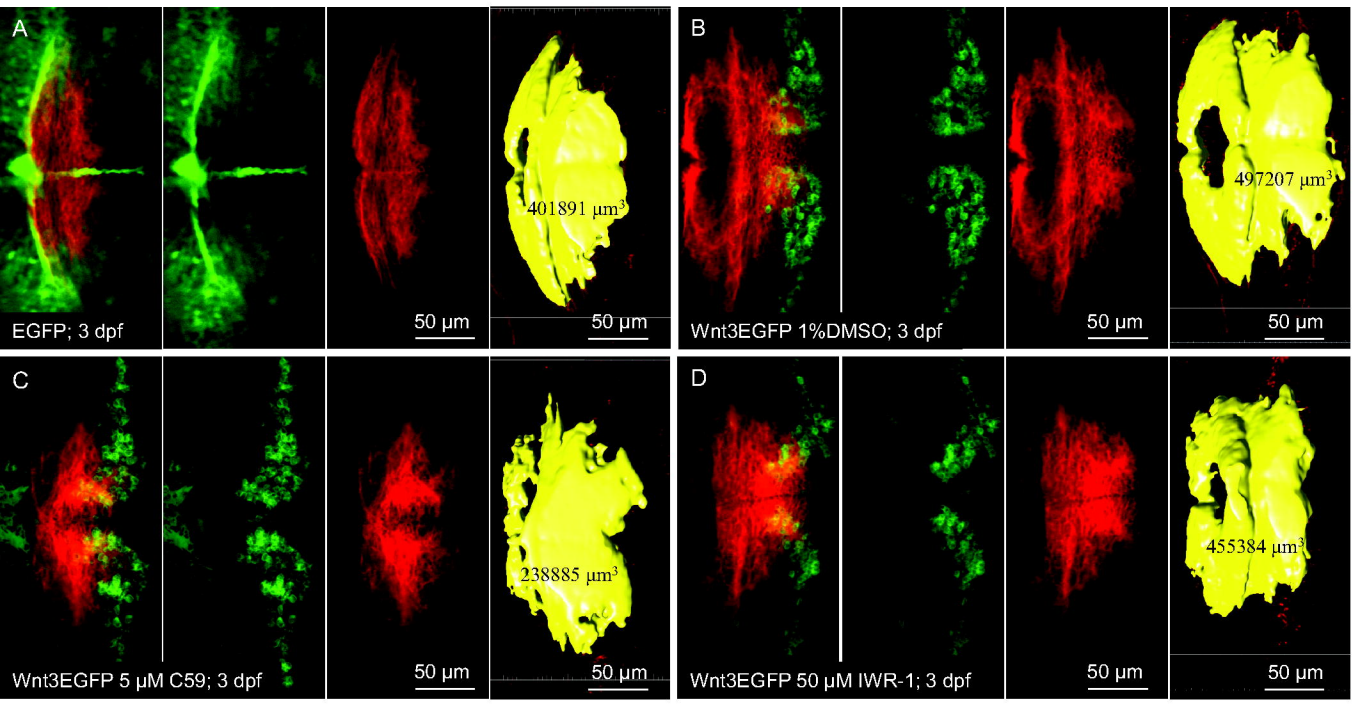

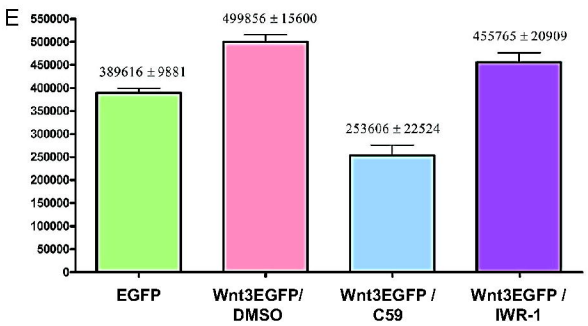

Fig. 8 - Teh et al.

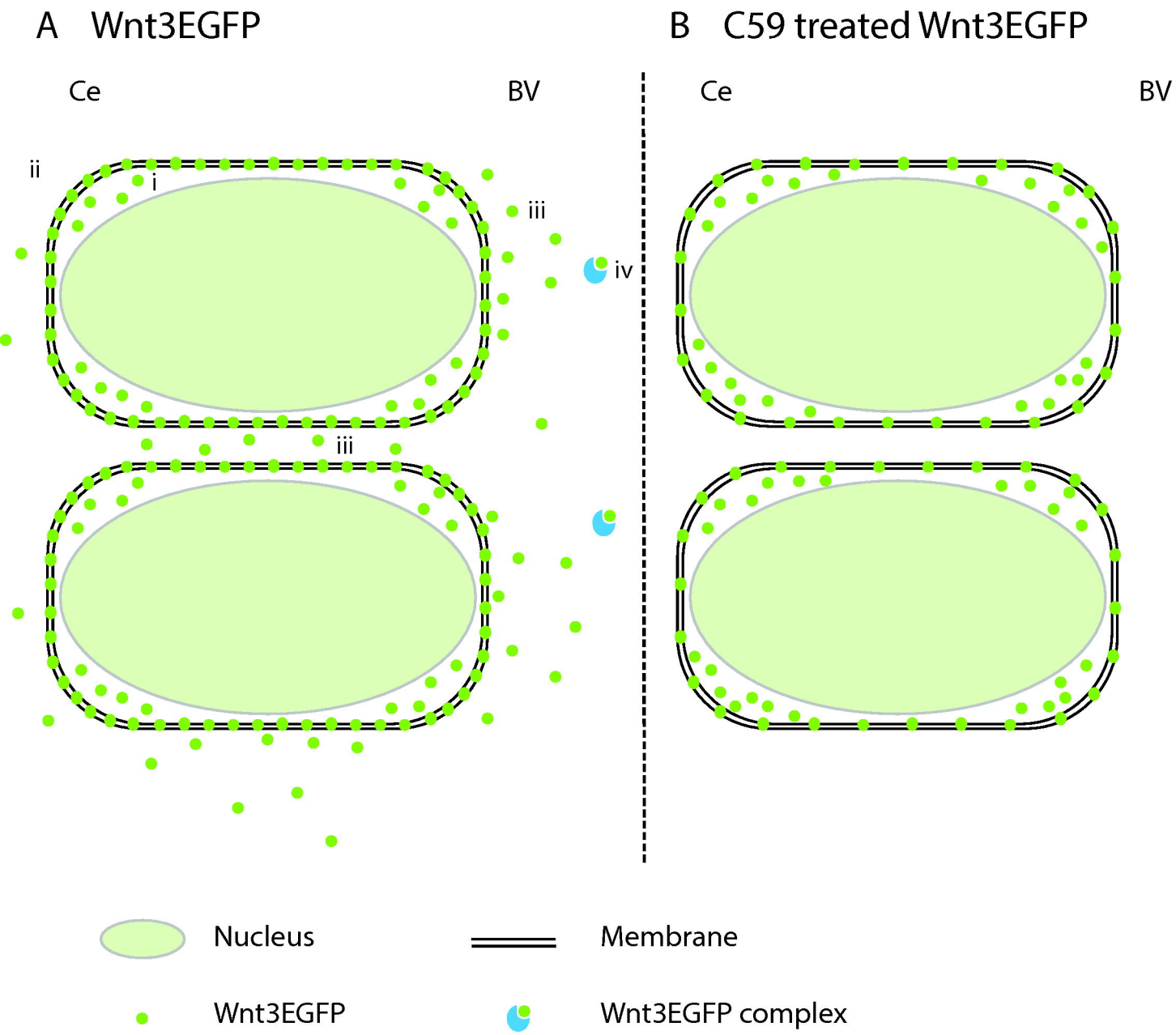

Fig. 9 - Teh et al.